

Utility of ultrasound superb microvascular imaging parameters for prediction of the initial effectiveness of monoclonal antibody therapy for cervical cancer

L. Zhang, H. Li, C. Guo, T. Cheng*

Changzhou Cancer Hospital, Changzhou City, Jiangsu province, China

ABSTRACT

► Original article

*Corresponding author:

Tao Cheng, M.D.,

E-mail:

chengtao1216@hotmail.com

Received: December 2024

Final revised: January 2025

Accepted: February 2025

Int. J. Radiat. Res., July 2025;
23(3): 619-625

DOI: 10.61186/ijrr.23.3.16

Keywords: Superb microvascular imaging, cervical cancer, monoclonal antibody, tislelizumab, bevacizumab.

Background: Globally, PD-1/PD-L1 inhibitors combined with bevacizumab have shown promising results in treating renal and lung cancers, but their efficacy in cervical cancer (CC) remains unclear. Superb microvascular imaging (SMI) is a novel technique for observing microcirculation in tumors. This study investigated the effectiveness and survival benefits of SMI in assessing tislelizumab combined with bevacizumab for treating CC. **Materials and Methods:** 86 patients with CC (2022–2023) were randomly divided into two groups: group A (bevacizumab, n=43) and group B (tislelizumab + bevacizumab, n=43). After 4 cycles of treatment, tumor volume and Adler blood-flow grades were assessed using color Doppler flow imaging (CDFI) and SMI. Receiver operating characteristic (ROC) curves were used to evaluate the diagnostic value of both methods in assessing treatment effects. **Results:** Both CDFI and SMI demonstrated significant differences in treatment effectiveness between groups ($p < 0.05$). CDFI showed improved Adler blood-flow grades after treatment in both groups ($p < 0.05$), but they were not significantly different between the groups ($P > 0.05$). SMI also revealed significant improvements ($p < 0.01$) and greater differences between groups after treatment ($p < 0.05$). The area under the curve (AUC) for SMI in evaluating therapeutic efficacy was 0.833 (sensitivity 86.05%, specificity 69.77%), while CDFI showed an AUC of 0.816 (sensitivity 79.07%, specificity 72.09%). **Conclusions:** Tislelizumab combined with bevacizumab significantly improves CC treatment. SMI outperforms CDFI in evaluating tumor microvessels and provides valuable insight for the planning of early CC treatment.

INTRODUCTION

Cervical cancer (CC) is a malignant neoplasm that originates from the squamous epithelial cells of the cervix and is one of the most common cancers in terms of both incidence and mortality among women. It is the fourth most frequently diagnosed malignant tumor in women worldwide ⁽¹⁾. According to national cancer statistics in China, CC has the second highest occurrence among malignant tumors among women behind only breast cancer, with 130,000 new cases reported each year, which account for 28% of all new CC cases globally ⁽²⁾.

In the early stages, clinical symptoms are often mild. With progress of the disease, vaginal contact bleeding, postmenopausal irregular vaginal bleeding, vaginal discharge, and other symptoms gradually appear. In late stages of the disease, extreme weight loss, dysuria, anemia, fatigue, and massive vaginal bleeding occur ⁽³⁾. Thus, early and precise diagnosis and therapy are crucial for CC.

The development of CC relies on the creation of new blood vessels. At present, color doppler flow imaging (CDFI) is frequently used to assess the neovascularization of tumors and can distinguish high-speed blood flow, but not actual low-speed blood flow and movement artifacts ^(4, 5). Superb microvascular imaging (SMI) is significantly superior to CDFI in evaluating micro vessels of malignant tumors ⁽⁶⁾. SMI is a newly developed color blood flow imaging technique based on the principle of CDFI and has high sensitivity and resolution. It can detect the dynamic status of low-velocity blood flow and microcirculation perfusion while retaining the subtle low-velocity blood-flow signals ⁽⁷⁻⁹⁾.

Targeted therapy targets a specific disease mechanism or biomarker to minimize damage to normal cells and improve efficacy and safety. The types of targeted anticancer drugs include vascular endothelial growth factor (VEGF) inhibitors, programmed death receptor-1/ programmed death molecule ligand-1 (PD-1/PD-L1) inhibitors, and

phosphatidylinositol-3 kinase (PI3K) inhibitors⁽¹⁰⁻¹²⁾. Various signaling pathways that mediate the onset of tumor development have received more attention than traditional tumor immunotherapy modalities, including PD-1/PD-L1⁽¹³⁾.

Tislelizumab is an immune checkpoint inhibitor that blocks the immune escape of tumors from T-cells and has shown good efficacy in a variety of tumors⁽¹⁴⁾. Bevacizumab is a kind of VEGF inhibitor that has the ability to prevent VEGF receptor binding, inhibit angiogenesis, and inhibit tumor spread. It has been widely used in clinical tumor treatment and has shown significant effectiveness in various cancer therapies⁽¹⁵⁾. Clinical studies have established bevacizumab as a first-line treatment in conjunction with platinum-based drugs, but the median overall survival for patients remains below 17 months⁽¹⁶⁾. Studies have indicated that elevated levels of PD-1/PD-L1 and inflammatory markers in the peripheral blood of patients with CC may result in immune suppression and facilitate tumor growth and metastasis⁽¹⁷⁾. Consequently, PD-1 or PD-L1 inhibitors to obstruct the PD-1/PD-L1 signaling pathway have emerged as a novel immunotherapy approach for CC.

Reports indicate that the combination of bevacizumab and the PD-L1 inhibitor atezolizumab can significantly enhance treatment effectiveness for metastatic, persistent, or recurrent CC in clinical practice⁽¹⁸⁻²⁰⁾. However, there is a lack of comprehensive studies using ultrasound SMI technique to assess the combination of bevacizumab and tislelizumab in the management of early-stage CC, and the potential mechanisms require further investigation. Therefore, we used CDFI combined with SMI for comprehensive treatment evaluation of lesion changes in patients with early CC to explore the relationship between hemodynamic parameters and the status of early CC. The results could provide a new reference for the evaluation of the efficacy of monotherapy in early CC.

MATERIALS AND METHODS

Participants

This prospective, randomized controlled trial evaluated tumor volume, blood flow changes, and the safety of CDFI combined with SMI in patients with early-stage CC receiving single and combined monoclonal antibody treatment. The inclusion criteria were the diagnostic criteria in clinical guidelines for CC⁽²¹⁾, clinical staging and grading of CC established by the International Federation of Gynecology and Obstetrics (FIGO)⁽²²⁾, and CC diagnosis by ultrasound-guided biopsy. All patients had complete SMI imaging data, CDFI imaging data, ultrasound data and histopathological examination results. All patients had not received any monoclonal antibody treatment before enrollment, and blood

counts, electrocardiograms, and liver and renal function tests were performed normally at admission. The exclusion criteria were pregnant or breastfeeding patients, other malignant tumors or other serious important functional organ diseases, receiving other CC monoclonal antibodies before treatment, and an inability to cooperate with clinical work due to intellectual disability or mental disorder.

Treatment plan

A total of 86 patients with early CC diagnosed and treated from 2022 to 2023 were selected, and their ages were 28–56 years. Eligible patients were randomly assigned to receive bevacizumab (group A, $n = 43$) or tislelizumab combined with bevacizumab (group B, $n = 43$) using stratified block randomization. Group A ($n = 43$) was treated with standard therapy, which consisted of intravenous cisplatin at 50 mg/m² or carboplatin with an area under the concentration curve (AUC) of 5 mg/mL/min combined with paclitaxel at 175 mg/m² and bevacizumab at 15 mg/kg. Group B ($n = 43$) was administered tislelizumab at 200 mg for standard treatment along with group A. The relevant drug informations are as follows: Cisplatin: norm: 2 mL: 10 mg; drug code: H20040812; China Jiangsu Haosen Pharmaceutical Group Co., Ltd. Carboplatin: norm: 10 mL: 100 mg, drug code: H20020180, China Qilu Pharmaceutical Co., Ltd. Paclitaxel: norm: 100 mg; drug code: H20183378, China Jiangsu Hengrui Medicine Co., Ltd. Bevacizumab: norm: 400 mg, drug code: S20120069, Switzerland Roche Pharma Ltd. Tislelizumab: norm: 100 mg; drug code: S20190045, China Guangzhou BeOne Medicines Co., Ltd. Both groups underwent treatment in cycles of 3 weeks, with administration occurring on the first day of each cycle for a total of 4 cycles. Treatment was discontinued if disease progression resulted in unacceptable toxic effects or the patient withdrew from the study.

Instruments and methods

The study was done using a Canon Aplio900 Doppler ultrasound diagnostic instrument (Japan Canon Medical System Co., Inc.) with a high-frequency probe (5–14 MHz) and scanning on the same plane. The measurements for each observation index were documented for both groups of patients before and after treatment. The patients were asked to empty their bladders prior to the examination and then assumed a supine position with a bent knee. The probe was inserted transvaginally for CDFI and SMI assessments.

The condition of the uterine adnexa was assessed with concentration on the shape, size, location, extent, distance from the edge, and total depth of cervix invasion. The area of exploration extended from the bladder neck to the rectal fossa and included the cervical ligament region. CDFI mode was used to assess the tumor's blood flow, and both CDFI and SMI

were conducted to visualize the tumor's vascular distribution.

The section with the greatest concentration of blood vessels in the tumor was identified while minimizing manual pressure on the tumor, allowing for observation of color blood flow within and surrounding the tumor. SMI mode was initiated concurrently. The segment with the highest vascularity was chosen for blood-flow signal analysis. After four cycles of treatment, the effectiveness of the two groups of monoclonal antibodies was assessed.

Efficacy evaluation

The tumor lesion volume was assessed based on the World Health Organization's criteria for evaluating responses in solid tumors⁽²³⁾. Complete response (CR) was characterized by the total disappearance of the tumor for over 4 weeks. Partial response (PR) was identified as a decrease in tumor volume greater than 50% compared to pre-treatment measurements for more than 4 weeks. Stable disease (SD) was defined as a reduction of less than 50% or an increase of 25% or less in tumor volume compared to baseline. Disease progression (PD) was indicated by an increase in tumor volume exceeding 25% or the emergence of new lesions.

CDFI and SMI were used to compare the minimum blood-flow velocities before and after treatment. The blood-flow signals from CDFI and SMI was graded according to the Adler grading system⁽²⁴⁾, where scores range from 0 to 3 and align with levels 0 to III. Grade 0 represents an absence of blood-flow signals, and grade I indicates a minimal blood-flow signal visible as two spots or thin short line signals. Grade II denotes a moderate blood-flow signal consisting of 3 to 4 spots or one longer vessel, and grade III reflects a significant blood-flow signal within the tumor showing more than 5 spots or over 2 elongated blood vessels.

To evaluate the efficacy of ultrasound, the curative effect after treatment was graded according to the tumor volume and blood-flow signal before and after treatment. Ultrasound grades of 0–1, 2–3, 4–5, and 6 points corresponded to CR, PR, SD, and PD, respectively. Clinical safety assessment was performed according to the side effects experienced by both groups following treatment, including nausea, vomiting, gastrointestinal issues, bone marrow suppression, leukopenia, and pain.

Statistical analysis

SPSS 26.0 (IBM Corporation, USA) was used for statistical analysis. The measurement data are represented as the mean \pm standard deviation ($\bar{x} \pm s$), and a paired-sample *t*-test was performed. The χ^2 test was used to analyze the count data and Adler blood-flow classification before and after the treatments. The therapeutic effect was assessed with CDFI and

SMI through a rank-sum test, and ROC curves were created. The AUC, 95% confidence interval (CI), sensitivity, and specificity were calculated to assess the validity of SMI in evaluating therapeutic outcomes. Values of *p* less than 0.05 indicated statistically significant differences.

RESULTS

Comparison of baseline characteristics

The baseline characteristics of the two groups of patients were compared. As shown in table 1, there were no significant differences in terms of age, FIGO stage and grading, and pathological type (*p*>0.05). This allowed for the discovery of variances that could be attributed to the intervention instead of differences in baseline characteristics among the groups.

Table 1. Comparison of baseline characteristics of the both groups.

Parameter			Group B (combination therapy)	Group A (monotherapy)	t/χ^2	P
n			43	43		
Age(year)			46.77± 11.98	41.19± 10.51	0.648	0.519
FIGO	I	A	26	28	0.199	0.655
		B	11	10	0.063	0.802
	II	A	6	5	0.104	0.747
		B	0	0		
	III	A	0	0		
		B	0	0		
	IV	A	0	0		
		B	0	0		
Pathological type	Squamous carcinoma		32	31	0.059	0.808
	Adenocarcinoma		9	11	0.261	0.610
	Other		2	1	0.345	0.557

CDFI evaluation

Table 2 shows the CDFI results of evaluating the therapeutic effectiveness of in terms of tumor volume. Group A had 1 case with CR, 15 cases with PR, 19 cases with SD, and 8 cases with PD. Group B had 2 cases with CR, 26 cases with PR, 10 cases with SD, and 2 cases with PD. The rank-sum test revealed a significant difference in efficacy assessment (*p*<0.05).

Table 2. Evaluation of the efficacy of color doppler flow imaging technique in the both groups after treatment.

Group	<i>n</i>	CR	PR	SD	PD	<i>Z</i>	<i>P</i>
Group B (combination therapy)	43	2	26	10	5	2.366	0.018
Group A(monotherapy)	43	1	15	19	8		

SMI evaluation

Table 3 shows the SMI results of the comparative study of the effectiveness in terms of tumor volume in the two groups. Group A had 3 cases of CR, 16 cases of PR, 18 cases of SD, and 6 cases of PD. Group B had 4 instances of CR, 29 instances of PR, 7 instances of SD, and 3 instances of PD. The rank-sum test indicated a significant difference in efficacy assessment (*p*<0.01).

Table 3. Evaluation of the efficacy of superb microvascular imaging technique in the both groups after treatment.

Group	n	CR	PR	SD	PD	Z	P
Group B (combination therapy)	43	4	29	7	3	2.687	0.007
Group A (monotherapy)	43	3	16	18	6		

CDFI method for blood-flow grading

Table 4 and figure 1 show the blood-flow grading before and after treatment (CDFI method) in both groups. Before treatment in Group B, the Adler blood-flow grading assessed by CDFI revealed grade 0 in 4 cases, grade I in 6 cases, grade II in 18 cases, and grade III in 15 cases. After treatment, the results indicated level 0 in 19 cases, level I in 8 cases, level II in 10 cases, and level III in 6 cases. Before treatment, Group A had grade 0 in 3 cases, grade I in 5 cases, grade II in 21 cases, and grade III in 14 cases. After treatment, the grading in this group was level 0 in 11 cases, level I in 13 cases, level II in 10 cases, and level III in 9 cases. The results demonstrated significant improvements after treatment in both groups ($p<0.05$). However, there were no significant differences in the Adler blood-flow grades after treatment ($\chi^2 = 3.924, p = 0.27, p>0.05$).

Table 4. Color doppler flow imaging Adler blood flow grading of the both groups.

Group	n		Grade 0	Grade I	Grade II	Grade III	χ^2	P
Group B (combination therapy)	43	Before treatment	4	6	18	15	16.211	<0.05
		After treatment	19	8	10	6		
Group A (monotherapy)	43	Before treatment	3	5	21	14	13.118	<0.05
		After treatment	11	13	10	9		

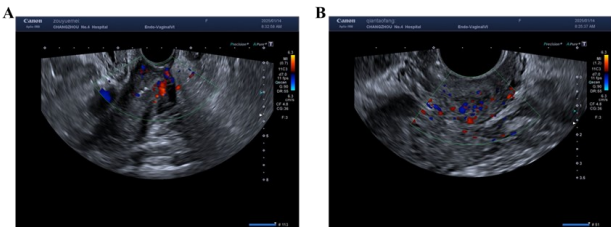


Figure 1. Blood flow grading charts in both groups. (A: Before treatment, B: After treatment).

SMI method for blood-flow grading

Table 5 and figure 2 show the blood-flow grading before and after treatment with the SMI method in both groups. Before treatment, the Adler blood-flow grading by SMI in group B indicated 0 cases of grade 0, 3 cases of grade I, 9 cases of grade II, and 31 cases of grade III. After treatment, group B had level 0 in 18 cases, level I in 9 cases, level II in 8 cases, and level III in 8 cases.

Before treatment, the grading assessed by SMI in group A indicated 0 cases of grade 0, 4 cases of grade I, 7 cases of grade II, and 32 cases of grade III. After treatment, this group showed level 0 in 10 cases, level I in 11 cases, level II in 11 cases, and level III in 11 cases. The results indicated that the Adler blood-

flow grades of both groups of patients assessed by SMI improved significantly compared with the pretreatment period ($p<0.01$). Additionally, there was a significant difference in the Adler blood-flow grades after treatment ($\chi^2 = 8.932, p = 0.03, p<0.05$).

Table 5. Superb microvascular imaging Adler blood flow grading of the both groups.

Group	n		Grade 0	Grade I	Grade II	Grade III	χ^2	P
Group B (combination therapy)	43	Before treatment	0	3	9	31	44.949	<0.01
		After treatment	21	11	6	5		
Group A (monotherapy)	43	Before treatment	0	4	7	32	23.979	<0.01
		After treatment	10	9	13	11		

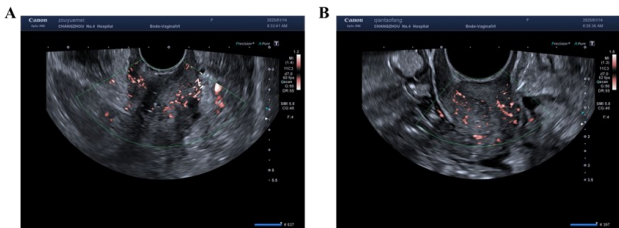


Figure 2. Blood flow grading charts in both groups (A: Before treatment, B: After treatment).

SMI and CDFI evaluation of therapeutic effects

Table 6 and figure 3 show the results of the impact of SMI and CDFI parameters on the treatment of CC. The findings indicated that the AUC of SMI was 0.833 (95% CI: 0.750–0.917) with 86.05% sensitivity and 69.77% specificity. In contrast, the AUC of CDFI was 0.816 (95% CI: 0.728–0.905) with 79.07% sensitivity and 72.09% specificity.

Table 6. The value of superb microvascular imaging and color doppler flow imaging in evaluating the therapeutic effect of cervical cancer.

	AUC	%95CI	Sensitivity %	Specificity %
SMI	0.833	0.917~0.750	86.05	69.77
CDFI	0.816	0.905~0.728	79.07	72.09

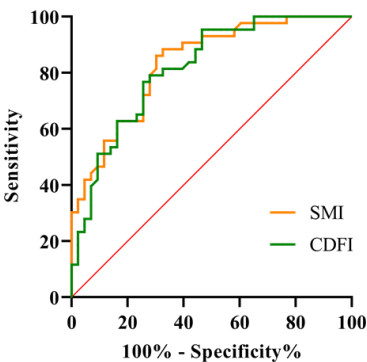


Figure 3. Analysis of the predictive value of superb microvascular imaging and color doppler flow imaging for treatment efficacy.

Comparisons of clinical safety

The occurrences of adverse reactions in both groups are shown in table 7. In group B, there were 25 instances of adverse reactions, while group A had 17 instances. There was no significant difference between the two groups ($p>0.05$).

Table 7. Comparison of clinical safety between the both groups after treatment.

	Nausea and vomiting	Gastrointestinal reactions	Bone marrow suppression	Leukopenia	Pain	Overall Incidence
Group B (combination therapy)	4	6	2	5	8	%58.14
Group A (monotherapy)	3	3	1	4	7	%39.53
χ^2	0.528					
P	0.971					

DISCUSSION

CC is one of the most prevalent malignancies among women ⁽²⁵⁾. Human papillomavirus (HPV) infection is the primary contributing factor to CC, and other associated risk factors include smoking, having multiple sexual partners, early onset of sexual activity, multiple pregnancy and fertility, and immunodeficiency diseases ^(26, 27). Recent statistics indicate that the incidence of CC is rising and showing a tendency to affect younger individuals ⁽²⁸⁾. In addition, in China, health awareness is insufficient, and many patients discover they are already in the advanced stages of CC by the time they experience discomfort. This results in missed opportunities for optimal treatment. Early CC can usually have a good prognosis if enough attention and corresponding treatment are provided ⁽²⁹⁾.

Studies have found that targeted therapy plays a key role in inhibiting tumor growth and can block the growth and spread of tumor cells by acting on at cells themselves or their surrounding microenvironment through specific mechanisms ⁽³⁰⁾. Ongoing advancements in targeted therapies and immunotherapies, particularly anti-angiogenic agents like bevacizumab, have substantially enhanced the survival rates of patients with CC ⁽³¹⁻³³⁾. Nevertheless, there has been no in-depth study on the therapeutic effects of their combination. The rate of complete pathological response could potentially be enhanced by assessing the effectiveness of the combination treatment of tislelizumab and bevacizumab, which could help to improve prognoses and holds significant implications for clinical practice.

With the wide application of targeted therapy in clinical practice, methods for assessing the effectiveness of monoclonal antibodies have increasingly drawn attention ⁽³⁴⁻³⁶⁾. For patients with CC, accurate evaluation of the efficacy of monoclonal antibody treatment is key to the formulation of subsequent treatment plans. At present, the commonly used therapeutic evaluation methods include cervical cytology, HPV tests, imaging evaluation, and pathological evaluation ⁽³⁷⁾. As imaging techniques advance, they have gained benefits of being non-invasive, convenient, and easily repeatable, which have led to growing adoption of imaging methods for evaluating the effectiveness of monoclonal antibody treatments for CC ⁽³⁸⁾.

The growth, proliferation, and spread of tumors are closely linked to the development of neovascularization, so reduction or disappearance of

blood-flow signals in tumor lesions has significance for the evaluation of therapeutic effects and prognosis ^(39, 40). The evaluation of blood-flow signals in primary lesions of CC is a major advantage of the CDFI technique ⁽⁴¹⁾. The findings indicated a significant difference in efficacy evaluation after treatment ($p < 0.05$). CDFI could show the arteries and veins with relatively high flow rate, and filtering could eliminate clutter and motion artifacts to obtain clear image data. At the same time, the Adler blood-flow grading assessed by CDFI revealed a notable improvement in both groups after treatment compared to before treatment ($p < 0.05$). The proportion of Adler blood-flow grades 0 and I increased significantly, and the proportion of grades II and III decreased significantly.

There was no significant difference in Adler blood-flow grade after treatment ($p > 0.05$). The findings are similar to those reported in the study by Han *et al.* on non-contrast microfluidic imaging to assess blood flow in liver tumors ⁽⁴²⁾. This suggests that CDFI can effectively reflect changes in the blood supply of tumor tissue before and after monoclonal antibody therapy. However, CDFI cannot show the low-velocity small neovascularization with diameter less than 0.2 mm, and its discrimination is poor when assessing neovascularization with low velocity or very low velocity, which may introduce some bias to the results.

The CDFI technique has obvious limitations in evaluating tumor microvessels, while the SMI technique has obvious advantages in terms of sensitivity to low-velocity blood flow and its ability to describe vascular morphology and distribution ^(6, 43). Compared with CDFI, SMI can show more microvessels, more intricate vascular structures, and both peripheral and central vascular distribution in CC ^(8, 41, 44). Research has indicated that SMI outperforms CDFI in assessing and defining vascular abnormalities in thyroid nodules, as well as investigating the diagnostic efficacy of vascular lesions. The formation of blood vessels in thyroid nodules detected by the SMI technique is one of the effective markers for identifying thyroid cancer ^(45, 46). Therefore, SMI can make up for the deficiencies of CDFI in the detection of microvessels and is more sensitive in detecting tumor neovascularization.

SMI imaging of branch vessels demonstrated greater precision and spatial resolution, indicating that the SMI technique has considerable advantages in detecting tumor neovascularization. The SMI findings revealed a significant difference in efficacy

evaluation after treatment ($p < 0.05$). In addition, the Adler blood-flow grading assessed by SMI after treatment showed a remarkable improvement compared to before treatment in both groups ($p < 0.05$). There was a significant increase in the proportions of grades 0 and I and a notable decline in grades II and III. The Adler blood-flow grading exhibited a significant difference after treatment ($p < 0.05$).

ROC curves were generated using the clinical outcomes of the two groups after treatment as a variable. The results indicated that the AUC of SMI for assessing the effectiveness of the two groups under various treatment protocols was 0.833 (95% CI: 0.750–0.917) with 86.05% sensitivity and 69.77% specificity. In comparison, the AUC of CDFI was 0.816 (95% CI: 0.728–0.905) with 79.07% sensitivity and 72.09% specificity. There was no notable difference in sensitivity and specificity between SMI and CDFI regarding the evaluation of CC, but SMI exhibited a higher AUC than CDFI. Chae *et al.* reported similar findings in their study on the added value of the vascular Index on SMI to assess breast masses ⁽⁴⁷⁾.

Both CDFI and SMI can be used to assess the effectiveness of monoclonal antibody therapy in CC, and each of them demonstrates a certain predictive value for treatment outcomes. They are dependable tools for monitoring patients with CC undergoing monoclonal antibody therapy that can help to provide noninvasive and simple observations of the condition of patients. Furthermore, they can guide the clinical adjustment of treatment plans in a timely manner and provide accurate information for the evaluation of the efficacy of monoclonal antibody treatment.

There are some limitations to this study. The sample size was relatively small, which may have led to biased findings and affected the extrapolation and reliability of the conclusions. In addition, the observation period was short. Long-term effects are crucial for comprehensive understanding of treatment effects and the development of scientific treatment strategies.

CONCLUSION

In conclusion, the combination of tislelizumab and bevacizumab has superior effectiveness in treating CC as assessed by SMI and CDFI compared to bevacizumab alone. This combination can reduce tumor size, enhance blood-flow signals, and offer more valuable insights for developing treatment strategies involving monoclonal antibodies for CC. The sample size of this study is limited, and in the future, it will be necessary to expand the sample size and have better control of human error to evaluate the reliability of this method more accurately.

ACKNOWLEDGMENT

None.

Consent to Participate: We secured a signed informed consent form from every participant.

Conflicts of Interest: The authors declare that they have no financial conflicts of interest.

Consent to Publish: The manuscript has neither been previously published nor is under consideration by any other journal. The authors have all approved the content of the paper.

Ethic Approval: This study was approved by Changzhou Cancer Hospital (Approval number: 2024 (SR) NO.024 Registration date: 2024.10.25).

Data Availability Statement: The data that support the findings of this study are available from the corresponding author, upon reasonable request.

Funding: None.

Author Contribution: L.Z.; Developed and planned the study. Edited and refined the manuscript with a focus on critical intellectual contributions. H.L.; Participated in collecting, assessing, and interpreting the data. Made significant contributions to data interpretation and manuscript preparation. C.G.; Performed experiments, and interpreted results. T.C.; Provided substantial intellectual input during the drafting and revision of the manuscript.

REFERENCES

- Moore DH (2006) Cervical cancer. *Obstetrics and gynecology*, **107** (5): 1152-61.
- Bray F, Laversanne M, Sung H, Ferlay J, Siegel RL, Soerjomataram I, *et al.* (2024) Global cancer statistics 2022: GLOBOCAN estimates of incidence and mortality worldwide for 36 cancers in 185 countries. *CA: a Cancer Journal for Clinicians*, **74**(3): 229-63.
- Gopu P, Antony F, Cyriac S, Karakasis K, Oza AM (2021) Updates on systemic therapy for cervical cancer. *The Indian Journal of Medical Research*, **154**(2): 293-302.
- Wen C, Huang L, Jiang H (2021) Diagnosis of Interventional transvaginal maternal diseases based on color doppler ultrasound. *Journal of Healthcare Engineering*, **2021**: 5517785.
- Yang Z, Cai J, Wang Y, Shu L, Liu W, Wang Z (2024) Comparison of doppler imaging and microvascular imaging in cervical lymph node blood flow analysis. *Current Medical Imaging*, **20**(1): e15734056306197.
- Zhu Y, Tang Y, Jiang Z, Zhang J, Jia S, Li Y, *et al.* (2023) Potential diagnostic value of quantitative superb microvascular imaging in premalignant and malignant cervical lesions. *Frontiers in Oncology*, **13**: 1250842.
- Zhu Y, Tang Y, Zhang G, Zhang J, Li Y, Jiang Z (2022) Quantitative analysis of superb microvascular imaging for monitoring tumor response to chemoradiotherapy in locally advanced cervical cancer. *Frontiers in Oncology*, **12**: 1074173.
- Zhong J, Huang L, Su M, Wu M, Lin X, Shui X, *et al.* (2023) Ultrasound microvessel visualization in cervical cancer: association between novel ultrasound techniques and histologic microvessel densities. *Ultrasound in Medicine & Biology*, **49**(12): 2537-47.
- Sato W, Suto Y, Yamanaka T, Watanabe H (2021) An advanced ultrasound application used to assess peripheral vascular diseases: superb microvascular imaging. *Journal of Echocardiography*, **19**(3): 150-7.
- Salomon-Perzyńska M, Perzyński A, Rembielak-Stawecka B, Michalski B, Skrzypulec-Plinta V (2014) VEGF--targeted therapy for the treatment of cervical cancer --literature review. *Ginekologia Polska*, **85**(6): 461-5.

11. Mezache L, Panicia B, Nyinawabera A, Nuovo GJ (2015) Enhanced expression of PD L1 in cervical intraepithelial neoplasia and cervical cancers. *Modern Pathology*, **28**(12): 1594-602.
12. Fu K, Zhang L, Liu R, Shi Q, Li X, Wang M (2020) MiR-125 inhibited cervical cancer progression by regulating VEGF and PI3K/AKT signaling pathway. *World Journal of Surgical Oncology*, **18**(1): 115.
13. Shen S, Hong Y, Huang J, Qu X, Sooranna SR, Lu S, et al. (2024) Targeting PD-1/PD-L1 in tumor immunotherapy: mechanisms and interactions with host growth regulatory pathways. *Cytokine & Growth Factor Reviews*, **79**: 16-28.
14. Zhang L, Geng Z, Hao B, Geng Q (2022) Tislelizumab: A modified anti-tumor programmed death receptor 1 antibody. *Cancer Control*, **29**: 1073274822111296.
15. Tewari KS, Sill MW, Long HJ, 3rd, Penson RT, Huang H, Ramondetta LM, et al. (2014) Improved survival with bevacizumab in advanced cervical cancer. *The New England Journal of Medicine*, **370**(8): 734-43.
16. Chuai Y, Rizzuto I, Zhang X, Li Y, Dai G, Otter SJ, et al. (2021) Vascular endothelial growth factor (VEGF) targeting therapy for persistent, recurrent, or metastatic cervical cancer. *The Cochrane Database of Systematic Reviews*, **3**(3): Cd013348.
17. Chen Z, Pang N, Du R, Zhu Y, Fan L, Cai D, et al. (2016) Elevated expression of programmed death-1 and programmed death ligand-1 negatively regulates immune response against cervical cancer cells. *Mediators of Inflammation*, **2016**: 6891482.
18. Oaknin A, Gladiéff L, Martínez-García J, Villacampa G, Takekuma M, De Giorgi U, et al. (2024) Atezolizumab plus bevacizumab and chemotherapy for metastatic, persistent, or recurrent cervical cancer (BEATcc): a randomised, open-label, phase 3 trial. *Lancet (London, England)*, **403**(10421): 31-43.
19. Friedman CF, Snyder Charen A, Zhou Q, Carducci MA, Buckley De Meritens A, Corr BR, et al. (2020) Phase II study of atezolizumab in combination with bevacizumab in patients with advanced cervical cancer. *Journal for Immunotherapy of Cancer*, **8**(2): e001126.
20. Lei J, Zhang J, You C, Liu M, Li N (2024) First-line treatment with atezolizumab plus bevacizumab and chemotherapy for US Patients with metastatic, persistent, or recurrent cervical cancer: a cost-effectiveness analysis. *Value in health*, **27**(11): 1528-1534.
21. de Juan A, Redondo A, Rubio MJ, García Y, Cueva J, Gaba L, et al. (2020) SEOM clinical guidelines for cervical cancer (2019). *Clinical & Translational Oncology*, **22**(2): 270-8.
22. Kido A and Nakamoto Y (2021) Implications of the new FIGO staging and the role of imaging in cervical cancer. *British Journal of Radiology*, **94**(1125): 20201342.
23. Gouda MA, Janku F, Wahida A, Buschhorn L, Schneeweiss A, Abdel Karim N, et al. (2024) Liquid biopsy response evaluation criteria in solid tumors (LB-RECIST). *Annals of Oncology*, **35**(3): 267-75.
24. Che D, Yang Z, Wei H, Wang X, Gao J (2020) The Adler grade by Doppler ultrasound is associated with clinical pathology of cervical cancer: Implication for clinical management. *PloS one*, **15**(8): e0236725.
25. Li H, Wu X, Cheng X (2016) Advances in diagnosis and treatment of metastatic cervical cancer. *Journal of Gynecologic Oncology*, **27**(4): e43.
26. Cohen PA, Jhingran A, Oaknin A, Denny L (2019) Cervical cancer. *Lancet (London, England)*, **393**(10167): 169-82.
27. Bedell SL, Goldstein LS, Goldstein AR, Goldstein AT (2020) Cervical Cancer screening: past, present, and future. *Sexual Medicine Reviews*, **8**(1): 28-37.
28. Buskwofe A, David-West G, Clare CA (2020) A review of cervical cancer: incidence and disparities. *Journal of the National Medical Association*, **112**(2): 229-32.
29. Somashekhar SP and Ashwin KR. (2015) Management of early-stage cervical cancer. *Reviews on Recent Clinical Trials*, **10**(4): 302-8.
30. Menderes G, Black J, Schwab CL, Santin AD (2016) Immunotherapy and targeted therapy for cervical cancer: an update. *Expert Review of Anticancer Therapy*, **16**(1): 83-98.
31. Bizzarri N, Ghirardi V, Alessandri F, Venturini PL, Valenzano Mena-da M, Rundle S, et al. (2016) Bevacizumab for the treatment of cervical cancer. *Expert Opinion on Biological Therapy*, **16**(3): 407-19.
32. Plummer C, Michael A, Shaikh G, Stewart M, Buckley L, Miles T, et al. (2019) Expert recommendations on the management of hypertension in patients with ovarian and cervical cancer receiving bevacizumab in the UK. *British Journal of Cancer*, **121**(2): 109-16.
33. Feng CH, Mell LK, Sharabi AB, McHale M, Mayadev JS (2020) Immunotherapy With radiotherapy and chemoradiotherapy for cervical cancer. *Seminars in Radiation Oncology*, **30**(4): 273-80.
34. Colombo N, Dubot C, Lorusso D, Caceres MV, Hasegawa K, Shapira-Frommer R, et al. (2021) Pembrolizumab for persistent, recurrent, or metastatic cervical cancer. *The New England Journal of Medicine*, **385**(20): 1856-67.
35. McNamara B, Chang Y, Mutlu L, Harold J, Santin AD (2023) Pembrolizumab with chemotherapy, with or without bevacizumab for persistent, recurrent, or metastatic cervical cancer. *Expert Opinion on Biological Therapy*, **23**(3): 227-33.
36. Nishio S, Yonemori K, Usami T, Minobe S, Yunokawa M, Iwata T, et al. (2022) Pembrolizumab plus chemotherapy in Japanese patients with persistent, recurrent or metastatic cervical cancer: Results from KEYNOTE-826. *Cancer Science*, **113**(11): 3877-87.
37. Voelker RA (2023) Cervical Cancer Screening. *JAMA*, **330**(20): 2030.
38. Haldorsen IS, Lura N, Blaakær J, Fischerova D, Werner HMJ (2019) What is the role of imaging at primary diagnostic work-up in uterine cervical cancer? *Current Oncology Reports*, **21**(9): 77.
39. Ahir BK, Engelhard HH, Lakka SS (2020) Tumor development and angiogenesis in adult brain tumor: Glioblastoma. *Molecular Neurobiology*, **57**(5): 2461-78.
40. Li X, Zhou J, Wang X, Li C, Ma Z, Wan Q, et al. (2023) New advances in the research of clinical treatment and novel anticancer agents in tumor angiogenesis. *Biomedicine & Pharmacotherapy*, **163**: 114806.
41. Cannella R, Pilato G, Mazzola M, Bartolotta TV (2023) New microvascular ultrasound techniques: abdominal applications. *La Radiologia Medica*, **128**(9): 1023-34.
42. Han H, Ji Z, Ding H, Zhang W, Zhang R, Wang W (2019) Assessment of blood flow in the hepatic tumors using non-contrast micro flow imaging: Initial experience. *Clinical Hemorheology Microcirculation*, **73**(2): 307-16.
43. Zhang XY, Cai SM, Zhang L, Zhu QL, Sun Q, Jiang YX, et al. (2022) Association between vascular index measured via superb microvascular imaging and molecular subtype of breast cancer. *Frontiers in Oncology*, **12**: 861151.
44. Senyuva I, Turan CO, Yuksel GY, Senturk S (2023) Superb microvascular imaging doppler technique in the evaluation of ovarian stromal vascularity in women with polycystic ovary syndrome. *JPMA*, **73**(10): 1992-6.
45. Li F, Sun W, Liu L, Meng Z, Su J (2022) The application value of CDFI and SMI combined with serological markers in distinguishing benign and malignant thyroid nodules. *Clinical & Translational Oncology*, **24**(11): 2200-9.
46. Jin H, Wang C, Jin X (2022) Superb microvascular imaging for distinguishing thyroid nodules: A meta-analysis (PRISMA). *Medicine*, **101**(24): e29505.
47. Chae EY, Yoon GY, Cha JH, Shin HJ, Choi WJ, Kim HH (2021) Added Value of the vascular index on superb microvascular imaging for the evaluation of breast masses. *Journal of Ultrasound in Medicine*, **40**(4): 715-23.

